

## Remotely Triggered Release from Magnetic Nanoparticles\*\*

By Austin M. Derfus, Geoffrey von Maltzahn, Todd J. Harris, Tasmia Duza, Kenneth S. Vecchio, Erkki Ruoslahti, and Sangeeta N. Bhatia\*

Multivalent nanoparticles have tremendous potential in the diagnosis and treatment of human disease.<sup>[1]</sup> Their multivalency allows simultaneous conjugation of targeting ligands to improve nanoparticle homing, polymers (e.g., polyethylene glycol (PEG)) to improve nanoparticle pharmacokinetics, as well as therapeutic drug cargo. Drug release from a nanoparticle surface has been accomplished by bonds that are sensitive to hydrolytic degradation<sup>[2]</sup> or pH;<sup>[3]</sup> however, complex release profiles that can be controlled from large distances (>10 cm) have not been achieved. Here, we describe a multifunctional nanoparticle that is: (1) multivalent, (2) remotely actuated, and (3) imaged non-invasively by magnetic resonance imaging. Superparamagnetic nanoparticles act as transducers to capture external electromagnetic energy at 350–400 kHz, which is not significantly absorbed by tissue, to disrupt hydrogen bonding between complementary oligonucleotides on demand. With a nucleic acid strand covalently linked to the nanoparticle, dye-labeled single stranded DNA (a model antisense therapeutic) self-assembles on the particle's surface, forming a tunable, heat-labile linker. The multifunctional nanoparticles are used to demonstrate remote, pulsatile release of a single species and multistage release of two species *in vitro*, as well as noninvasive imaging and remote actuation upon implantation *in vivo*.

Release from surfaces or polymers triggered by an external stimulus (electric current,<sup>[4,5]</sup> magnetic fields,<sup>[6]</sup> temperature,<sup>[7,8]</sup> light,<sup>[9]</sup> ultrasound<sup>[10]</sup>) has been extensively studied (reviewed in<sup>[11]</sup>). These strategies, however, have been principally applied to macro- and micro-scale materials and drug reservoirs. For focal diseases, such as cancer, these devices must be implanted at the tumor site (e.g., Gliadel). Another approach is to replace these larger depots with drug-carrying nanoparticles that can be individually targeted to the tumor. Heat<sup>[12]</sup> and light-sensitive<sup>[13]</sup> liposomes, for example, can be delivered systemically and their contents released in response to an external stimulus. Our strategy has the added advantage of radiofrequency electromagnetic field (EMF) activation, which improves penetration depth over heat or light (at 400 kHz, field penetration into 15 cm of tissue is > 99 %<sup>[14]</sup>). Similarly, energy absorption, and thus background heating, of water and tissue is insignificant in the 350–400 kHz frequency regime.<sup>[15]</sup> In contrast, when applied to magnetic materials, these fields produce heat as the magnetic dipole of the material aligns with the external field.<sup>[16,17]</sup> We conjugated a 30 bp DNA to dextran-coated iron oxide nanoparticles and added a complement of 12, 18, or 24 bp linked to a model drug, a fluorophore. Excess fluorescent DNA was removed by trapping the particle on a magnetic column and washing with buffer. Particles were trapped in a matrigel plug as an *in vitro* model of tumor tissue, allowing fluorescent DNA to diffuse out into the surrounding buffer only when liberated from the particles. In Figure 1B we demonstrate pulsatile release of a fluorophore initiated by EMF pulses (400 kHz, 1.25 kW) of 5 min duration every 40 min. The fluorescence of the surrounding buffer increased markedly in the sampling immediately after EMF application, followed by a fluorescence decrease in subsequent samplings. Because much of the fluorescent DNA re-hybridized to the particles upon cooling of the plug to room temperature, subsequent EMF application allowed further release. Such a profile would be useful for metronomic dosing of a cytotoxic drug.<sup>[18]</sup>

The use of a nucleic acid duplex as a heat-labile linker adds the additional feature of temperature tunability through changes in chain length and variations in G/C content. Using a variable-gain RF amplifier to control particle heating, biomolecules tethered to these oligonucleotides can be released in multiple stages. In Figure 1C we use oligonucleotides of two different lengths and corresponding fluorescent species (12 bp, FAM; 24 bp, HEX) to demonstrate the potential for complex release profiles. Low power EMF pulses (0.55 kW) triggered release predominantly of FAM by melting of the

[\*] Prof. S. N. Bhatia,<sup>[†]</sup> Dr. A. M. Derfus, G. von Maltzahn,<sup>[†]</sup> T. J. Harris<sup>[†]</sup>  
Department of Bioengineering, University of California  
San Diego, CA (USA)  
E-mail: sbhatia@mit.edu

Dr. A. M. Derfus, Dr. T. Duza, Prof. E. Ruoslahti<sup>[††]</sup>  
Burnham Institute of Medical Research  
La Jolla, CA (USA)

Prof. K. S. Vecchio  
Department of NanoEngineering, Jacobs School of Engineering  
University of California  
San Diego, CA (USA)

[†] Current address: Harvard-M.I.T. Division of Health Sciences and Technology, Division of Electrical Engineering and Computer Science, Massachusetts Institute of Technology, and Division of Medicine, Brigham & Women's Hospital, 77 Massachusetts Ave. E19-502D, Cambridge, MA 02139, USA.

[††] Current address: Burnham Institute for Medical Research at University of California, Santa Barbara, CA 93106-9610, USA.

[\*\*] The authors thank Miriam Scadeng for MR imaging and acknowledge financial support of the David and Lucile Packard Foundation, the National Cancer Institute of the National Institutes of Health (N01-C0-37117, U54 CA119349-01, U54 CA119335, 1 R01 CA124427-01). AMD thanks the UC Biotechnology Research and Education Program for a G.R.E.A.T. fellowship (#2004-16). The authors declare no competing financial interests.

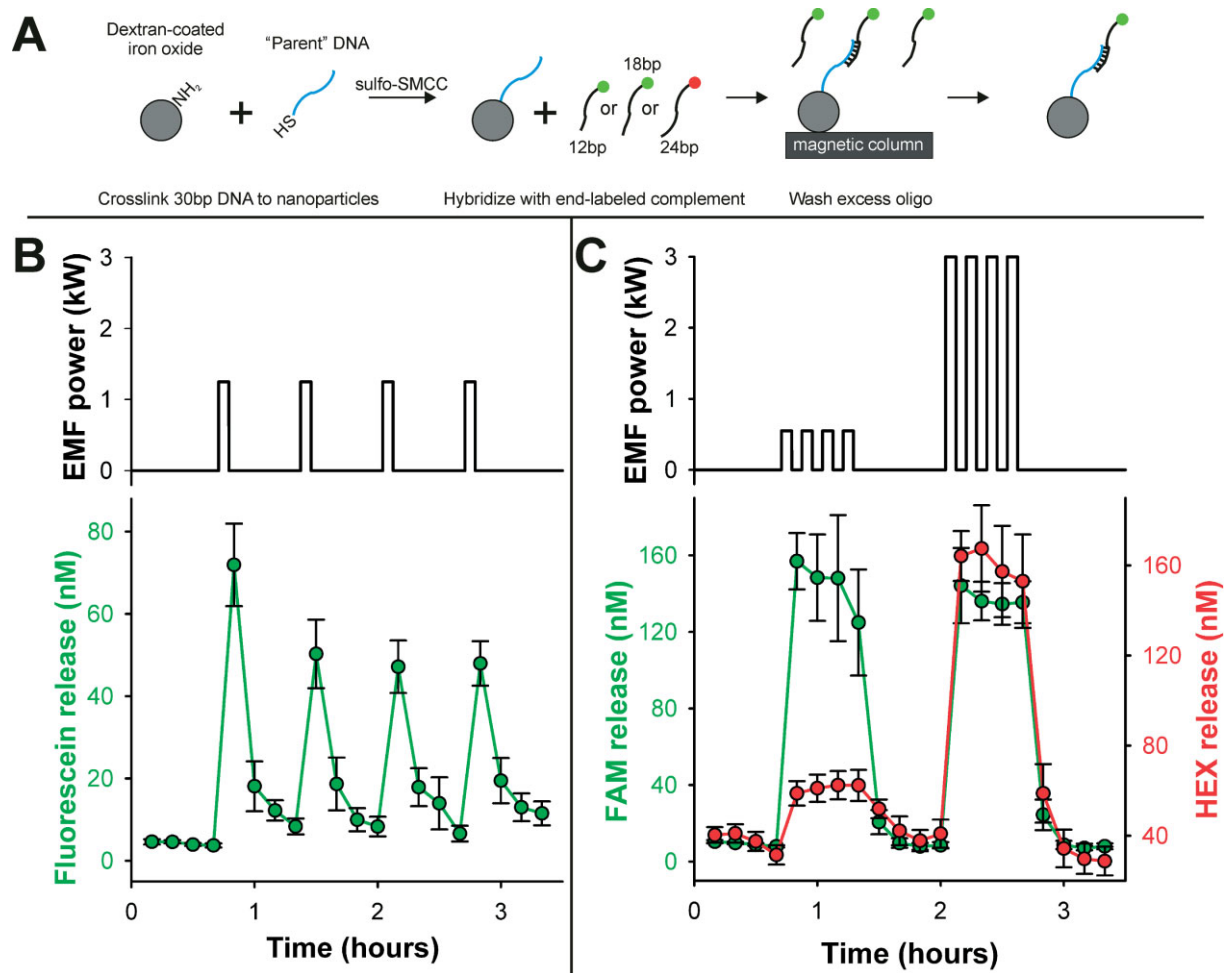


**Figure 1.** Electromagnetic field (EMF) triggered release of nanoparticle-tethered dye in pulsatile and multistage profiles. A) Particles were assembled by first covalently linking a 30 bp “parent” strand to a dextran-coated, iron oxide superparamagnetic nanoparticle, and then allowing a fluorescent complement (of 12, 18, or 24 bp) to hybridize. B) In vitro, nanoparticles hybridized to fluorescein-conjugated 18 bp were embedded in hydrogel plugs. Repeated EMF pulses of 5 minutes resulted in corresponding release of fluorescein. Alteration of oligonucleotide duplex length shifts response of heat-labile tether enabling complex, tunable release profiles. Low power EMF exposure results in release of FAM-conjugated 12 bp whereas higher power results in simultaneous melting of both 12 bp and 24 bp tethers (C).

12 bp complement whereas higher power (3 kW) led to simultaneous release of both species. Such a profile could be used to release multiple drugs in series, synergistic drug combinations such as a chemosensitizer and chemotherapeutic, or combination regimens such as antiangiogenic and cytotoxic compounds.<sup>[19]</sup>

This release scheme relies on sufficient temperature rise in vivo to initiate the DNA melting. While heating sufficient to trigger release cannot be attained at the single particle level ( $\Delta T \sim 10^{-5} \text{ }^\circ\text{C}$ ),<sup>[20]</sup> accumulation of a critical mass at a tumor site allows remote triggering through EMF application. It is therefore of interest to determine the nanoparticle concentrations required to heat various tumor diameters. Using an EMF setup and iron oxide formulation, we experimentally determined the relationship between temperature rise, particle concentration and sample diameter (Fig. 2) and fit these results to a conductive heat transfer model derived from Four-

ier’s law.<sup>[20]</sup> We determined that heating to  $42 \text{ }^\circ\text{C}$  in vivo would require  $\sim 1.2 \text{ mg}$  particles in a 1 cm diameter spherical tumor. These data serve as an upper bound on the potential for collateral heating as the model is based on steady-state temperature rise- shorter heating intervals can be used to generate steeper temperature gradients between the tumor and surrounding tissue. For release to occur, elevated temperatures are only required for short time periods, as DNA oligonucleotides disassociate tens of microseconds after sufficient heat is applied.<sup>[21]</sup> Our experiments show that reducing heating interval from 5 minutes to 30 seconds significantly reduces collateral heating (not shown); however, achieving a similar temperature rise with a shorter heating interval requires higher particle concentrations or increased EMF strength.

Next, we explored the use of the multifunctional nanoparticles in vivo by implantation of a subcutaneous model tumor consisting of a matrigel plug containing nanoparticles in living

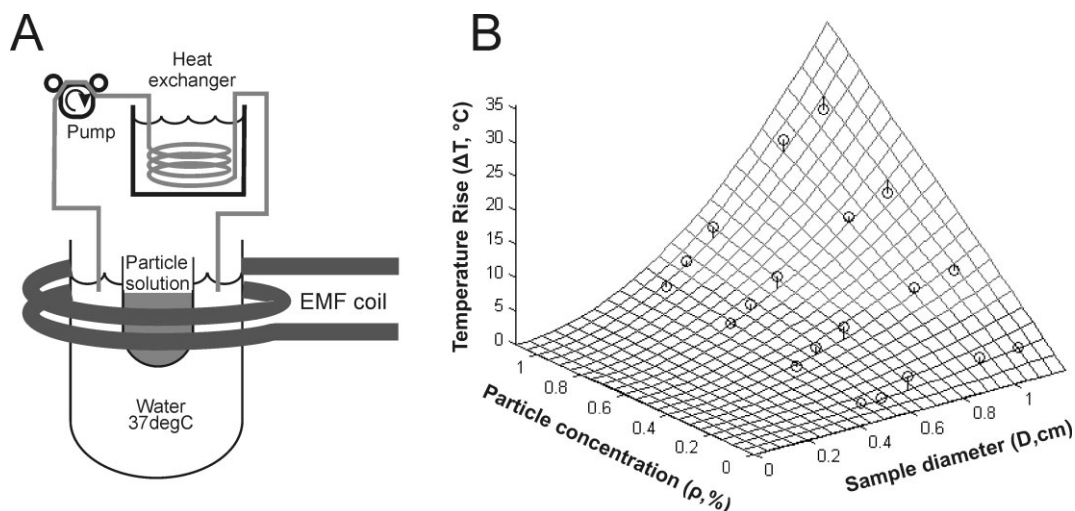


**Figure 2.** EMF-induced temperature rise varies with particle concentration and sample diameter. A) Experimental data was collected by applying maximum EMF (3 kW power) to solutions of various diameters  $D$  containing various concentration of magnetic particles ( $\rho$ ). B) These data (open circles) were fit to a conductive heat transfer equation  $\Delta T = \frac{q\rho D^2}{36k}$ , where  $k$  is thermal conductivity (for water:  $0.64 \text{ W m}^{-1} \text{ }^\circ\text{C}^{-1}$ ), and  $q$  is the heating rate ( $\text{mW mg}^{-1}$ ). With a threshold of  $5 \text{ }^\circ\text{C}$  temperature rise to trigger release, these results estimate a minimum of  $1.2 \text{ mg}$  particles must be delivered to a  $1 \text{ cm}$  diameter tumor.

mice. We examined the release of a fluorescein-labeled 18 bp oligonucleotide by EMF exposure of 3 kW and 5 min. After EMF treatment, tissue surrounding the model tumor was removed and examined for the presence of released dye. Fluorescent micrographs of histological sections in Figure 3B and C depict a dramatic increase in penetration depth of the model cargo into surrounding tissue due to EMF exposure. Image analysis was performed on 24 fluorescent images from each

group (3 animals, 8 images each). The average distance of fluorescence signal from the tissue/implant boundary in animals treated with EMF was approximately six-fold over unexposed controls ( $250 \pm 11$  vs.  $42 \pm 3 \text{ } \mu\text{m}$ , mean $\pm$ SEM). Such an increase in penetration depth could prove useful for treatment of the tumor periphery – areas often underdosed in hyperthermia generated by thermal seeds.<sup>[22]</sup> For deep-seated tumors, the use of EMF energy to break bonds remotely is an advan-

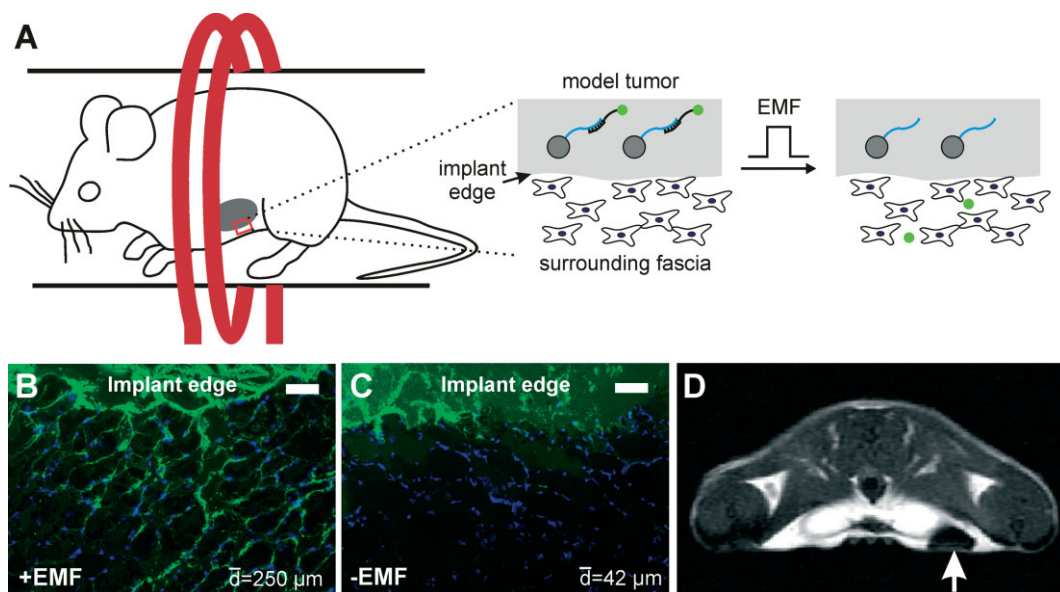


**Figure 3.** Remotely triggered release from nanoparticles in vivo. Nanoparticles were mixed with matrigel and injected subcutaneously near the posterior mammary fat pad of mice, forming model tumors (A). Application of EMF to implants containing 18 bp tethers resulted in release of model drugs and penetration far into surrounding tissue (B) when compared to unexposed controls (C, scale bar = 100 micrometers). These mice were imaged with a 7T MRI scanner, and transverse section shown in (D) depicts image contrast due to presence of nanoparticles (arrow).

tage over near-infrared light and other potential triggers that are more efficiently absorbed or scattered by tissue.<sup>[23]</sup> In addition to facilitating remote actuation, the magnetic particle core allows noninvasive visualization by MRI, as depicted in Figure 3D, suggesting the potential for simultaneous diagnosis and therapeutic delivery.

In our view, the fabrication of integrated, multifunctional nanodevices offers the potential to shift the current paradigm whereby diagnostics and therapeutics are sequential elements of patient care. In this example, nanoparticles could be delivered intravascularly using homing peptides,<sup>[24]</sup> used to visualize diseased tissue by MRI and then to guide focused application of electromagnetic energy, ultimately enabling remote, physician-directed drug delivery with minimal collateral tissue exposure. Instrumentation to apply high power, kHz-frequency fields to human patients is under development<sup>[25]</sup> and the performance of our remote actuation platform can be improved in the future by new materials and chemistry. Particle cores with higher magnetization would result in greater heating efficiency, requiring a lower particle concentration for release. Additionally, an improved heat-labile tether, with a sharp temperature transition slightly above 37 °C, might be obtained by attaching several duplexes in parallel,<sup>[26]</sup> and non-native nucleic acids may be used to mitigate the potentially deleterious effects of tissue nucleases. Despite the many promising avenues of further development presented above, the existing platform presented here demonstrates the ability to remotely trigger release of a biomolecule from the surface of a nanoparticle in vivo, thereby validating a 'modular' capability that can be adapted to improve the multifunctionality of a plethora of other nanomaterial formulations (e.g., near-infrared heating of gold nanoshells<sup>[23]</sup> and carbon nanotubes<sup>[27]</sup>).

## Experimental

**Particle Preparation:** Synthetic 30 bp 'parent' DNA (5'-Thiol-GAA GTG CGG TTA GTC GGC TTG AAT CAG CGA) was conjugated to 50 nm aminated magnetite nanoparticles (dextran-coated, Micro-mod), using sulfo-SMCC (Sigma) as the crosslinker. As the particles were found to contain  $\sim 10^4$  amine groups by fluorescamine assay, a 1000x excess of DNA was used in a two step reaction. Particles were first reacted with crosslinker for 1 h, filtered on a magnetic column (Miltenyi Biotec) to remove excess crosslinker, added to reduced DNA, and reacted overnight. After filtration of unconjugated parent DNA using a magnetic column, fluorescent complement DNA was added to the particles (in PBS) and allowed to hybridize overnight. The sequences used in these experiments were as follows (5' to 3'): 24 bp complement (CGC TGA TTC AAG CCG ACT AAC CGC), 18 bp complement (TGA TTC AAG CCG ACT AAC), 12 bp complement (TCG CTG ATT CAA). Dye conjugations were performed by the DNA supplier and occurred at the 5' end of the oligonucleotides. After hybridization, particles were filtered on a magnetic column at 4 °C to remove unbound complement.

**Model Tumor Preparation:** Phenol red free, growth factor reduced matrigel (400  $\mu$ L, BD Biosciences) was added to 100  $\mu$ L of particles. To obtain 1.05 % total concentration of particles, 75  $\mu$ L of DNA-conjugated particles ( $\sim 3.3$  mg mL<sup>-1</sup>) were added to 25  $\mu$ L of similar 50 nm particles (200 mg mL<sup>-1</sup>, Chemicell). Gels (total volume 500  $\mu$ L) were mixed at 4 °C to prevent gelation.

**In Vitro Experiments:** For in vitro experiments, gels were added to polypropylene microcentrifuge tubes and incubated at 37 °C for 45 min to allow gelation. Gel plugs were then washed three times with 500  $\mu$ L of PBS over 15 min. Buffer (200  $\mu$ L) was added to the plugs, and sampled and replaced with fresh buffer at 10 min intervals. When treated with EMF during a time interval, fields were switched on for 5 min only, preceded by  $\sim 2.5$  min and followed by  $\sim 2.5$  min at room temperature. When fields were not applied during an interval, samples remained at room temperature. Supernatant samples were assayed on a plate-reader fluorometer (Molecular Devices Gemini XS) and amount of DNA quantified with standards.

**In Vivo Experiments:** Prior to injection of matrigel plugs into mice, approval from the Burnham Institute Animal Use Committee was obtained (AUF 05-054). In these experiments, 500  $\mu$ L volumes were injected subcutaneously near the posterior mammary fat pad of six athymic nude mice and allowed to gel for 45 min. Prior to injection, animals were anesthetized with Avertin (tribromoethanol) and remained under anesthesia during the remainder of the experiment. Three animals were treated with EMF for two 5 min doses, with 15 min between field applications (+EMF), while three were not treated (-EMF). For treatment, mice were placed inside a plastic tube, which was mounted inside a horizontal two-turn copper coil. One hour after EMF treatment, animals were sacrificed. Model tumors and surrounding tissue (fascia and skin) were removed and embedded in OTC for histology. Sections were stained with DAPI and an anti-fluorescein antibody (followed by fluorescein conjugated secondary) to amplify small signals. To quantify penetration depth, 8 images of the tissue/implant boundary were taken for each animal (3 animals per group, 24 images total). DAPI staining was used to demarcate the boundary between the two regions. Using Metamorph software (Universal Imaging), green fluorescence on the tissue side of the boundary was quantified. For each fluorescent "object", the area and distance from the tissue boundary was measured. An area-weighted average distance was calculated.

**Radiofrequency Electromagnetic Field Applicator:** A 3 kW induction heating power supply (Ameritherm Nova 3) was used with a remote heating station and custom-made coils. The coil for in vitro experiments was 2.5 turns, 12 mm ID, and resonated at 400 kHz. For the heat transfer model and mice experiments, a 2-turn, 30 mm OD coil resonating at 338 kHz was used. All coils were constructed from 4.88 mm OD copper tubing and spray-coated with insulating paint. During experiments, cooling water (10–16 °C) was circulated through the coil.

**MR Imaging:** T1-weighted data sets of mice implanted with iron oxide particle containing gel plugs were acquired using a horizontal bore 7-Tesla imaging spectrometer (General Electric). T1-weighted acquisition was intended to achieve good anatomical detail. Data were acquired using a custom small animal imaging coil. Imaging parameters included a spin echo sequence, TR 500, TE 12, 40 mm field of view, matrix 256  $\times$  256, slice thickness 0.5 mm.

Received: January 11, 2007

Revised: June 18, 2007

- [1] M. Ferrari, *Nat. Rev. Cancer* **2005**, *5*, 161.
- [2] R. Gref, Y. Minamitake, M. T. Peracchia, V. Trubetskoy, V. Torchilin, R. Langer, *Science* **1994**, *263*, 1600.
- [3] N. Kohler, C. Sun, J. Wang, M. Zhang, *Langmuir* **2005**, *21*, 8858.
- [4] I. C. Kwon, Y. H. Bae, S. W. Kim, *Nature* **1991**, *354*, 291.
- [5] J. T. Santini, Jr., M. J. Cima, R. Langer, *Nature* **1999**, *397*, 335.
- [6] E. R. Edelman, J. Kost, H. Bobeck, R. Langer, *J. Biomed. Mater. Res.* **1985**, *19*, 67.
- [7] A. Chilkoti, M. R. Dreher, D. E. Meyer, D. Raucher, *Adv. Drug Delivery Rev.* **2002**, *54*, 613.
- [8] B. Jeong, S. W. Kim, Y. H. Bae, *Adv. Drug Delivery Rev.* **2002**, *54*, 37.
- [9] E. Mathiowitz, M. D. Cohen, *J. Membr. Sci.* **1989**, *40*, 67.

- [10] J. Kost, K. Leong, R. Langer, *Proc. Natl. Acad. Sci. USA* **1989**, *86*, 7663.
- [11] J. T. Santini, A. C. Richards, R. Scheidt, M. J. Cima, R. Langer, *Angew. Chem. Int. Ed.* **2000**, *39*, 2397.
- [12] D. Needham, M. W. Dewhirst, *Adv. Drug Delivery Rev.* **2001**, *53*, 285.
- [13] P. Shum, J. M. Kim, D. H. Thompson, *Adv. Drug Delivery Rev.* **2001**, *53*, 273.
- [14] J. H. Young, M. T. Wang, I. A. Brezovich, *Electron Lett* **1980**, *16*, 358.
- [15] P. R. Stauffer, T. C. Cetas, R. C. Jones, *IEEE Trans. Biomed. Eng.* **1984**, *31*, 235.
- [16] A. Jordan, P. Wust, H. Fahling, W. John, A. Hinz, R. Felix, *Int. J. Hyperther.* **1993**, *9*, 51.
- [17] R. Hergt, W. Andra, C. G. d'Ambly, I. Hilger, W. A. Kaiser, U. Richter, H. G. Schmidt, *IEEE Trans. Magn.* **1998**, *34*, 3745.
- [18] D. Hanahan, G. Bergers, E. Bergsland, *J. Clin. Invest.* **2000**, *105*, 1045.
- [19] S. Sengupta, D. Eavarone, I. Capila, G. Zhao, N. Watson, T. Kiziltepe, R. Sasisekharan, *Nature* **2005**, *436*, 568.
- [20] Y. Rabin, *Int. J. Hyperthermia* **2002**, *18*, 194.
- [21] A. Ansari, S. V. Kuznetsov, Y. Shen, *Proc. Natl. Acad. Sci. USA* **2001**, *98*, 7771.
- [22] I. Hilger, R. Hiergeist, R. Hergt, K. Winnefeld, H. Schubert, W. A. Kaiser, *Invest. Radiol.* **2002**, *37*, 580.
- [23] L. R. Hirsch, R. J. Stafford, J. A. Bankson, S. R. Sershen, B. Rivera, R. E. Price, J. D. Hazle, N. J. Halas, J. L. West, *Proc. Natl. Acad. Sci. USA* **2003**, *100*, 13549.
- [24] M. E. Akerman, W. C. Chan, P. Laakkonen, S. N. Bhatia, E. Ruoslahti, *Proc. Natl. Acad. Sci. USA* **2002**, *99*, 12617.
- [25] U. Gneveckow, A. Jordan, R. Scholz, V. Bruss, N. Waldofner, J. Ricke, A. Feussner, B. Hildebrandt, B. Rau, P. Wust, *Med. Phys.* **2004**, *31*, 1444.
- [26] R. Jin, G. Wu, Z. Li, C. A. Mirkin, G. C. Schatz, *J. Am. Chem. Soc.* **2003**, *125*, 1643.
- [27] N. W. Kam, M. O'Connell, J. A. Wisdom, H. Dai, *Proc. Natl. Acad. Sci. USA* **2005**, *112*, 11600.